Supplementary Information

Syngap1 and the development of murine neocortical progenitor cells

Soraia Barão[1,3,4,5]*, Yijun Xu[1], Ingie Hong[1,2,6,7]*, Ulrich Müller[1] and Richard L. Huganir[1,2]*

Included in this file are:

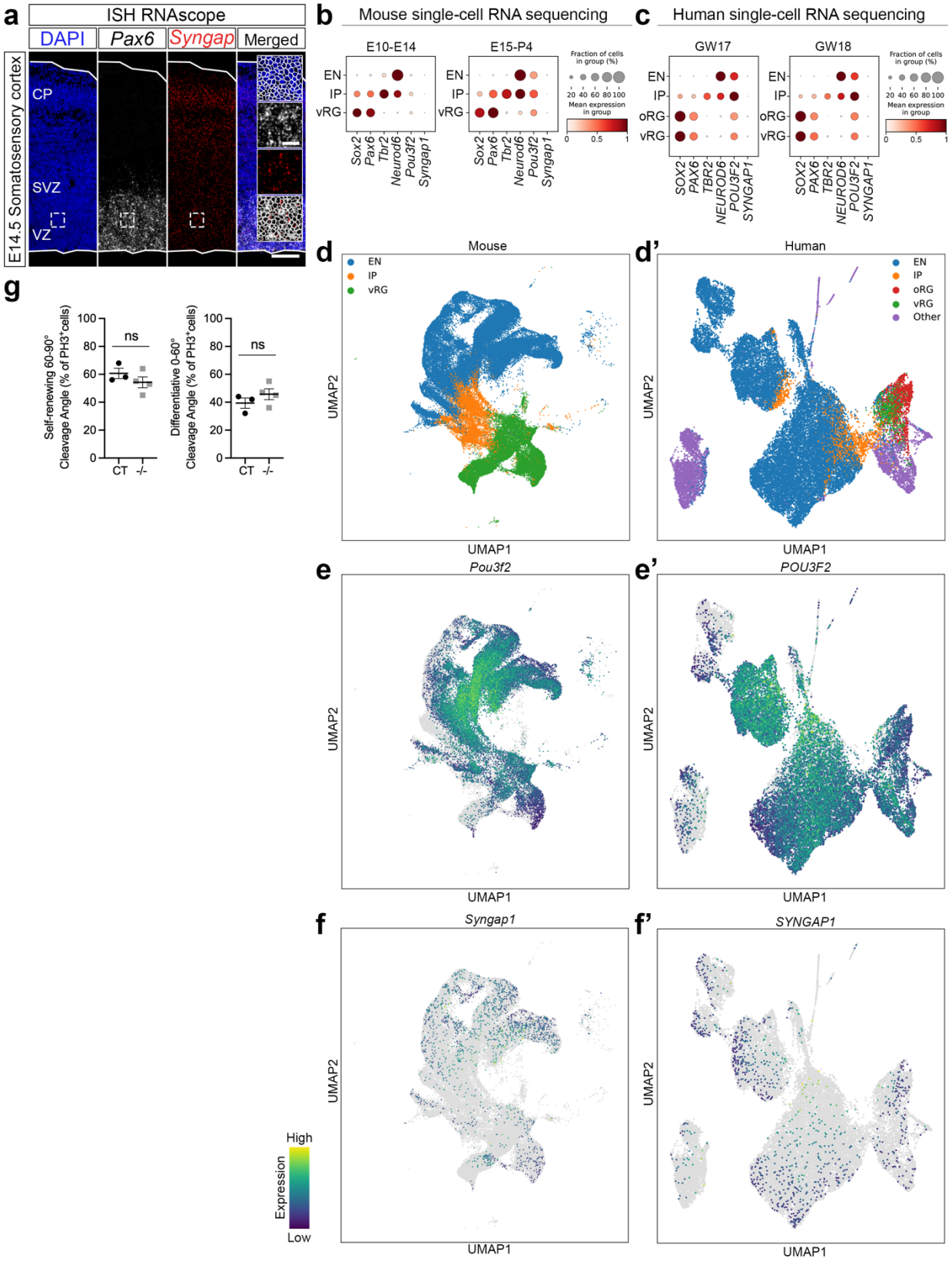
a
ISH RNAscope
DAPI
Pax6
Syngap
Merged
E14.5 Somatosensory cortex
CP
SVZ
VZ
b
Mouse single-cell RNA sequencing
E10-E14
E15-P4
EN
IP
vRG
Sox2
Pax6
Tbr2
Neurod6
Pou3f2
Syngap1
Fraction of cells in group (%)
Mean expression in group
c
Human single-cell RNA sequencing
GW17
GW18
oRG
SOX2
PAX6
TBR2
NEUROD6
POU3F2
SYNGAP1
g
Self-renewing 60-90° Cleavage Angle (% of PH3+cells)
Differentiative 0-60° Cleavage Angle (% of PH3+cells)
ns
CT
-/-
d
Mouse
d'
Human
Other
UMAP1
UMAP2
e
Pou3f2
e'
POU3F2
f
Syngap1
f'
SYNGAP1
High
Expression
Low

Supplementary Figure 1. *Syngap1* expression in mouse and human neocortex and mouse progenitors' cleavage plane analysis at E14.5. a RNAscope for *Syngap1* (red) and *Pax6* (grey) in the somatosensory cortex of wild-type mice at E14.5. Low and top lines represent the limits of the ventricular zone (VZ) and cortical plate (CP), respectively. Boxed area at higher magnification on the right. Lines circulating the cells show co-expression *Syngap1* and *Pax6* in the VZ. These results were confirmed in three independent mice. **b, c** Expression of cell marker genes (*Sox2*, *Pax6* = vRG; *Tbr2* = IP, *Neurod6* = EN), *Pou3f2* and *Syngap1* from previously published single-cell RNA sequencing analysis in mouse neocortex[31] (**b**) from embryonic age 10 (E10) to postnatal day 4 (P4) and human neocortex[32] (**c**) from gestational age 17 to 18 (GW17, GW18) represented as dotplots. **d, d'** UMAP of cell identities from single-cell RNA sequencing analysis in mouse neocortex[31] (**d**) and human neocortex[32] (**d'**). vRG, ventricular radial glial cells; oRG, outer radial glial cells; IP, intermediate progenitor cells; EN, excitatory neurons. **e-f'** UMAP of gene expression for *Pou3f2* (**e**) and *Syngap1* (**f**) in mouse neocortex and for POU3F2 (**e'**) and SYNGAP1 (**f'**) in human neocortex. **g** Cleavage plane analysis in Control (CT) and homozygous (-/-) *Syngap1KO* ventricular zone (VZ) at E14.5 (n=3 CT, n=4 -/- mice; two-sided unpaired *t*-test: CT vs -/- p=0.3010). SVZ, Subventricular Zone. Values are mean ± SEM; ns, not significant; Scale bars: 50 μm (lower magnification), 10 μm (higher magnification). Source data are provided as a Source Data file.

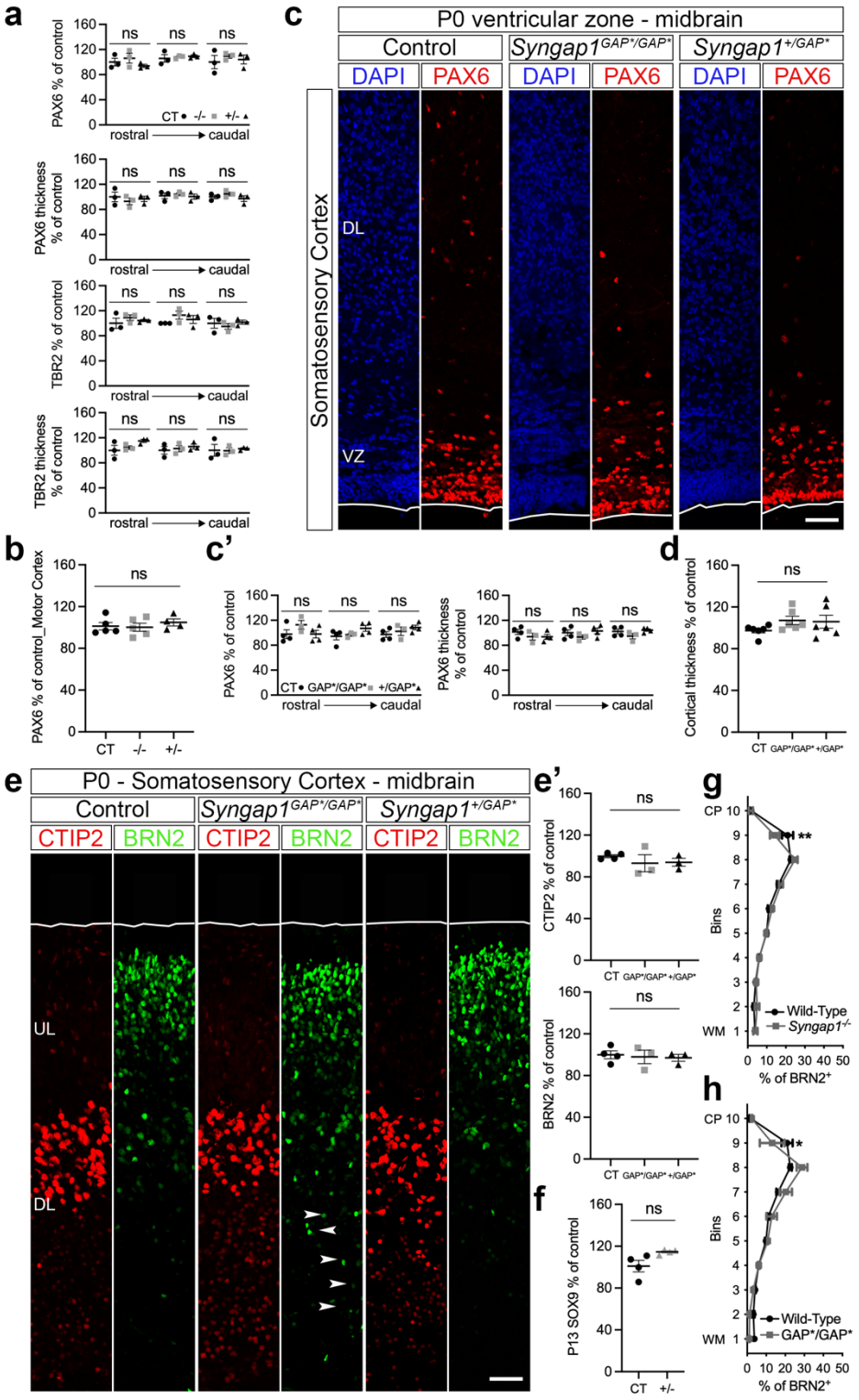

Supplementary Figure 2. *Syngap1* levels or activity do not affect the number, properties or output of progenitor cells in mice. a PAX6^{+} and TBR2^{+} cells quantification along the rostral-

caudal axis in Control (CT), heterozygous (+/-) and homozygous (-/-) *Syngap1KO* somatosensory cortex at E18.5 (related to Fig. 1c; n=3 mice/genotype; one-way ANOVA Dunnett's multiple comparisons test: $PAX6^+$ cells: rostral – CT vs -/- p=0.6974, CT vs +/- p=0.7080, $F_{2,6} = 1.063$; middle – CT vs -/- p=0.8805, CT vs +/- p=0.7600, $F_{2,6} = 0.2097$; caudal – CT vs -/- p=0.6115; CT vs +/- p=0.9035, $F_{2,6} = 0.3868$; $PAX6^+$ cortical thickness: rostral – CT vs -/- p=0.6268, CT vs +/- p=0.8982, $F_{2,6} = 0.3635$; middle – CT vs -/- p=0.8582, CT vs +/- p=0.9546, $F_{2,6} = 0.2666$; caudal – CT vs -/- p=0.5852, CT vs +/- p=0.8256, $F_{2,6} = 1.071$; $TBR2^+$ cells: rostral – CT vs -/- p=0.4438, CT vs +/- p=0.8039, $F_{2,6} = 0.6886$; middle – CT vs -/- p=0.2206, CT vs +/- p=0.6551, $F_{2,6} = 1.507$; caudal – CT vs -/- p=0.7577, CT vs +/- p=0.9652, $F_{2,6} = 0.3994$; $TBR2^+$ cortical thickness: rostral – CT vs -/- p=0.7756, CT vs +/- p=0.1352, $F_{2,6} = 2.346$; middle – CT vs -/- p=0.8963, CT vs +/- p=0.6375, $F_{2,6} = 0.3484$; caudal – CT vs -/- p=0.9978, CT vs +/- p=0.9360, $F_{2,6} = 0.074$). **b** $PAX6^+$ cells quantification in Control (CT), heterozygous (+/-) and homozygous (-/-) *Syngap1KO* motor cortex at E18.5 (n=5 CT and -/-, n=4 +/- mice; one-way ANOVA Dunnett's multiple comparisons test: CT vs -/- p=0.9694; CT vs +/- p=0.7277, $F_{2,11} = 0.4151$). **c** PAX6 (red) immunolabeling in the somatosensory cortex of Control (CT), heterozygous (+/*GAP**) and homozygous (*GAP*/GAP**) mice for *GAP-AL* mutation (*Syngap1GAP**) at P0. **c'** $PAX6^+$ cells quantification along the rostral-caudal axis in the somatosensory cortex of Control (CT), heterozygous (+/*GAP**) and homozygous (*GAP*/GAP**) mice for *GAP-AL* mutation (*Syngap1GAP**) at P0 (n=4 CT and +/*GAP**, n=3 *GAP*/GAP** mice; one-way ANOVA Dunnett's multiple comparisons test: $PAX6^+$ cells: rostral – CT vs *GAP*/GAP** p=0.2862, CT vs +/*GAP** p>0.9999, $F_{2,8} = 1.426$; middle – CT vs *GAP*/GAP** p=0.9322, CT vs +/*GAP** p=0.1552, $F_{2,8} = 2.070$; caudal – CT vs *GAP*/GAP** p=0.7101, CT vs +/*GAP** p=0.2182, $F_{2,8} = 1.436$; $PAX6^+$ cortical thickness: rostral – CT vs *GAP*/GAP** p=0.4443, CT vs +/*GAP** p=0.3684, $F_{2,8} = 1.051$; middle – CT vs *GAP*/GAP** p=0.5285, CT vs +/*GAP**

p=0.8415, $F_{2,8}$ = 1.106; caudal – CT vs *GAP*/GAP** p=0.2683, CT vs +/*GAP** p=0.8547, $F_{2,8}$ = 2.098). **d** Cortical thickness in the somatosensory cortex of Control (CT), heterozygous (+/*GAP**) and homozygous mice for *GAP-AL* mutation (*Syngap1GAP**) at P0 (n=4 CT and +/*GAP**, n=3 *GAP*/GAP** mice; one-way ANOVA Dunnett's multiple comparisons test: CT vs *GAP*/GAP** p=0.2431, CT vs +/*GAP** p=0.3277, $F_{2,15}$ = 1.406). **e, e'** CTIP2 (red) and BRN2 (green) immunolabeling in the somatosensory cortex of Control (CT), heterozygous (+/*GAP**) and homozygous (*GAP*/GAP**) mice at P0 (n=4 CT, n=3 *GAP*/GAP** and +/*GAP** mice; one-way ANOVA Dunnett's multiple comparisons test: CTIP2 – CT vs *GAP*/GAP** p=0.3848, CT vs +/*GAP** p=0.1743, $F_{2,7}$ = 0.6471; BRN2 – CT vs *GAP*/GAP** p=0.9357, CT vs +/*GAP** p=0.8712, $F_{2,7}$ = 0.1095). Arrowheads highlight migration defects for BRN2-positive cells. **f** SOX9 quantification in the somatosensory cortex of Control (CT) and *Syngap1*$^{+/-}$ mice at P13 (n=4 mice/genotype; two-sided unpaired t-test: CT vs +/- p=0.0528). **g, h** Distribution of BRN2^{+} cells in the somatosensory cortex of Control (CT), *Syngap1*$^{-/-}$ (**g**; related to Fig. 3a) and *Syngap1*$^{GAP*/GAP*}$ (**h**; related to Supplementary Fig. 2e) mice at P0 (n=4 CT and *Syngap1*$^{-/-}$, n=3 *Syngap1*$^{GAP*/GAP*}$ mice; two-way ANOVA-Šídák's multiple comparisons test: *Syngap1*$^{-/-}$ – 9-p=0.0017, $F_{9,60}$=2.236; *Syngap1*$^{GAP*/GAP*}$ – 9-p=0.0415, $F_{9,50}$=2.116). DL, Deep Layer; UL, Upper Layer; VZ, Ventricular Zone; WM, White Matter. Values are mean ± SEM; ns, not significant. Scale bars: 50 μm (P0), 100 μm (P13). Source data are provided as a Source Data file.

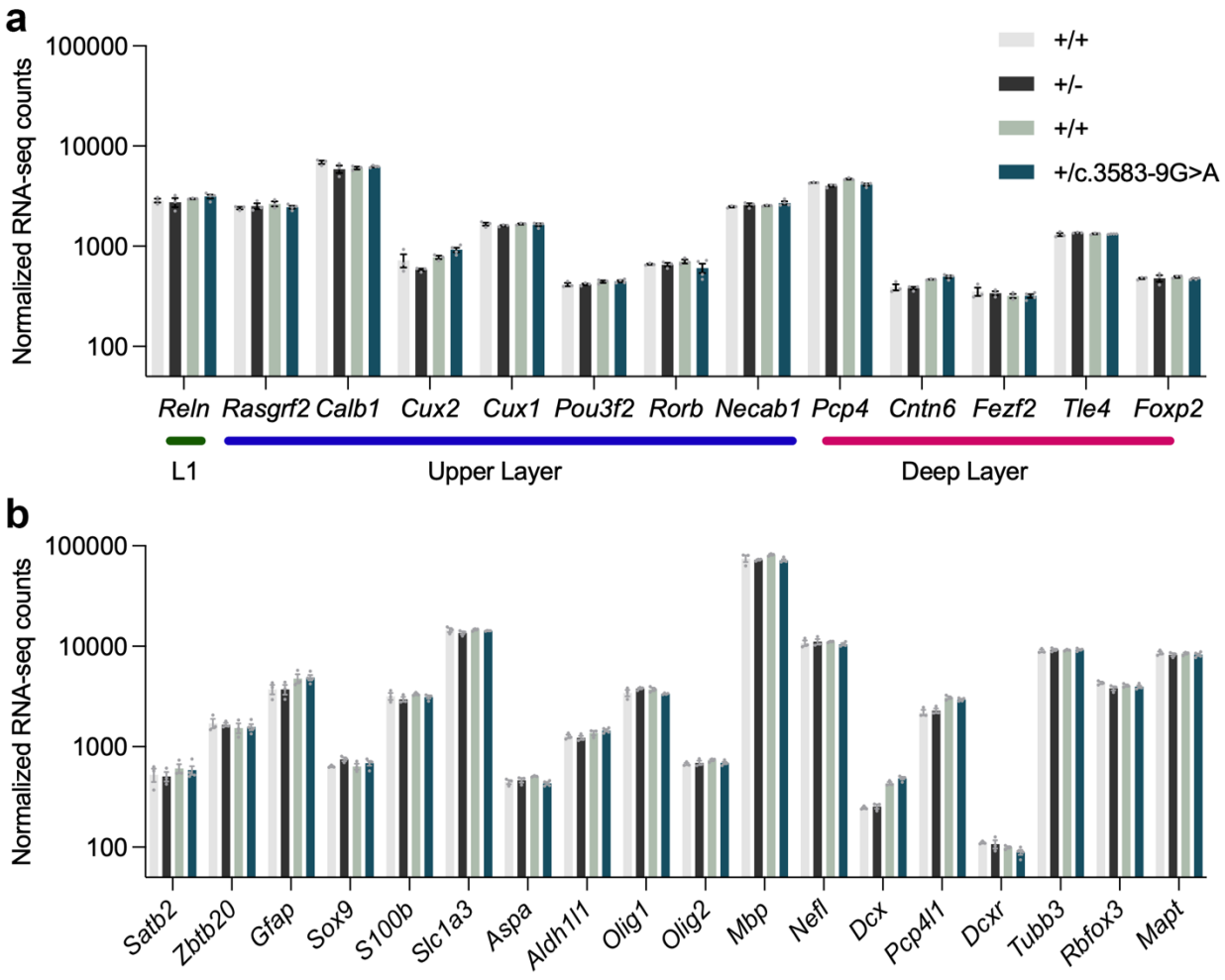

Supplementary Figure 3. Expression of neurodevelopmental marker genes in whole-brain RNA sequencing reveals no difference in two different *Syngap1* haploinsufficiency mouse models. **a** Layer-specific marker gene expression showed no difference (p_{adj} > 0.3 for all comparisons) in *Syngap1*$^{+/-}$ and *Syngap1*$^{+/c.3583\text{-}9G>A}$ mouse models, in comparison to respective wild-type littermate controls. **b** Markers for callosal projection neurons, glial cells, neurons, and axons also did not show significant differences (p_{adj} > 0.7 for all comparisons). Whole-mouse brain bulk RNA sequencing results from Araki et al. 2023[16] were reanalyzed and DESeq2 normalized counts were plotted for each marker gene. Source data are provided as a Source Data file.